

Luminescence of Eu ions in $\text{Al}_x\text{Ga}_{1-x}\text{N}$ across the entire alloy composition range

K. Wang,^{1,*} K. P. O'Donnell,¹ B. Hourahine,¹ R. W. Martin,¹ I. M. Watson,² K. Lorenz,³ and E. Alves³

¹*Department of Physics, SUPA, University of Strathclyde, Glasgow G4 0NG, Scotland, United Kingdom*

²*Institute of Photonics, SUPA, University of Strathclyde, Glasgow G4 0NW, Scotland, United Kingdom*

³*Instituto Tecnológico e Nuclear, Estrada Nacional 10, 2686-953 Sacavém, Portugal*

(Received 24 March 2009; revised manuscript received 18 July 2009; published 23 September 2009)

Photoluminescence (PL) and PL excitation (PLE) spectra of Eu-implanted $\text{Al}_x\text{Ga}_{1-x}\text{N}$ are obtained across the whole alloy composition range. The dominant ${}^5\text{D}_0$ - ${}^7\text{F}_2$ emission band broadens and then narrows as x increases from 0 to 1 while the peak shifts monotonically. This behavior is surprisingly similar to the broadening of excitons in a semiconductor alloy caused by composition fluctuations [E. F. Schubert *et al.*, Phys. Rev. B **30**, 813 (1984)]. PLE spectra reveal a steplike $\text{Al}_x\text{Ga}_{1-x}\text{N}$ band-edge absorption and two “subgap” bands $\text{X}_{1,2}$: X_1 peaks at 3.26 eV in GaN and shifts linearly to 3.54 eV in AlN. For $x > 0.6$, X_2 emerges approximately 1 eV higher in energy than X_1 and shifts in a similar way. We propose that $\text{X}_{1,2}$ involve creation of core-excitonic complexes of Eu emitting centers.

DOI: [10.1103/PhysRevB.80.125206](https://doi.org/10.1103/PhysRevB.80.125206)

PACS number(s): 78.55.Et, 71.35.-y, 71.20.Eh

I. INTRODUCTION

Photoluminescence (PL) spectroscopy of rare earth (RE) dopants in semiconductors has a long history.¹ Favennec *et al.*² reported that materials with wider band gaps show luminescence at higher temperatures (less quenching). Advances in growth technology led to RE doping of III-nitride epitaxial samples in the late 1990s, mainly GaN, eventually producing electroluminescent diodes and optically pumped lasers.³ $\text{Al}_x\text{Ga}_{1-x}\text{N}$ alloys, with band gaps from 3.4 to 6.2 eV, seem to offer advantages over GaN: however, Wakahara reported that $\text{Al}_x\text{Ga}_{1-x}\text{N}:\text{Eu}^{3+}$ luminescence efficiency improves as the AlN fraction x increases from 0 to ~ 0.3 but decreases at higher values of x .⁴ Lee and Steckl⁵ and Hömmerich *et al.*⁶ had earlier reported similar behavior for $\text{Al}_x\text{Ga}_{1-x}\text{N}:\text{Tm}$ with maximum emission in the range $0.6 < x < 0.8$. Current spectroscopic models of RE ions in solids derive from descriptions of free $4f$ states, with large spin-orbit coupling, perturbed by crystal fields. On this basis, atomic term identifiers have been assigned to experimental emission lines.⁷ The relatively small perturbations due to host-ion interactions play an essential role in *enabling* luminescence, by relaxing selection rules.⁸ However, the search for chemical trends in the values of the several parameters that quantify the interaction has had very mixed results.⁷ At the same time, there is confusion regarding the mechanism of excitation energy transfer from extended to localized states at light-emitting centers in RE-doped semiconductors. The emphasis here has been either on the atomic properties of RE ions⁹ or on the defect physics of the hosts.¹⁰ Aligning the energy levels of the RE ions with the band diagram of the host⁹ corresponds to a model of excitation via charge transfer from nearest neighbors (ligands) to the RE $4f$ shell. An Auger-type process has also been proposed, involving the nonradiative transfer of energy released from band-band recombinations in the host to the RE ions.¹¹ An alternative description regards the RE^{3+} ion as an isoelectronic trap, which localizes a carrier; the charged center subsequently binds a carrier of opposite sign to form a localized exciton, which then excites the $4f$ shell.¹⁰ Excitation models that require a further “RE-

related defect,” which may be a “carrier trap,”¹² to mediate the excitation process, also feature in the literature.¹³ In this paper we demonstrate that aspects of both “atomic properties” and “defect physics” descriptions are important to describe the RE luminescence and attempt to present a simplified description of the phenomenology. Our excitation model for $\text{Al}_x\text{Ga}_{1-x}\text{N}:\text{Eu}^{3+}$ formally equates charge transfer with isoelectronic exciton creation and thus avoids the need for sensitizing defects. The entire sharp-line emission is ascribed to the annihilation of excitons at Eu ions. Similar experimental findings for Dy-, Tm-, and Pr-doped samples^{14,15} suggest that excitonic processes feature strongly in the optical processes of light-emitting RE-doped nitrides generally. The possibility of direct excitation of higher RE levels should also be considered. A recent report describes direct excitation of higher-lying Tm³⁺ states that appear within the host gap for higher AlN fractions.¹⁶

II. EXPERIMENTAL DETAILS

A series of $\text{Al}_x\text{Ga}_{1-x}\text{N}$ samples with low AlN molar fractions ($x \leq 0.22$) was grown by metal organic vapor phase epitaxy (MOVPE) in an AIXTRON 200/4 RF-S reactor on (0001) sapphire substrates. Layers approximately 700 nm thick were deposited on 1.2- μm -thick GaN buffers on sapphire. Another series of $\text{Al}_x\text{Ga}_{1-x}\text{N}$ layers with higher AlN fractions ($0.07 \leq x \leq 1$) was obtained from Technologies and Devices International Inc. These samples, nominally 500 nm thick, were grown directly on (0001) sapphire substrates by hydride vapor phase epitaxy. An additional $\text{Al}_{0.98}\text{Ga}_{0.02}\text{N}$ sample (S1), especially grown by MOVPE, was included in the set.¹⁷ Details of the full sample set are provided in Table I. Eu ions were implanted into each sample to a fluence of 1×10^{15} at/cm² along the surface normal with a beam energy of 300 keV. Post-implantation annealing was performed in N_2 at temperatures from 1000 to 1300 °C for 20 min. One sample was treated by rapid thermal annealing (RTA) at 1420 °C for 2 min in flowing N_2 . All samples were protected using an unimplanted AlN proximity cap in order to inhibit out diffusion of nitrogen during annealing. A thin epitaxial

TABLE I. AlN molar fractions, measured by WDX and RBS, and annealing temperatures for the Eu-implanted $\text{Al}_x\text{Ga}_{1-x}\text{N}$ samples. Eu ions were implanted along the surface normal (*c* axis) with 1×10^{15} at/cm² at 300 keV.

Sample	AlN fraction (%)		Anneal temperature (°C)
	WDX (%)	RBS (%)	
StrGaN35	0	0	1300
Str397	9		1200
Str391	11		1200
Str395a	13		1100
Str395b	14		1200
Str398a	15		1200
Str396	16		1200
Str398b	21		1300
Str414	22		1200
TDI1	7		1200
TDI2a	31		1300
TDI2b	31	30	1420 (RTA)
TDI3		60	1300
TDI4		74	1300
TDI5		100	1300
S1		98	1300

AlN capping layer additionally protects the GaN sample.¹⁸ The compositions of the low-*x* samples were measured by wavelength dispersive x-ray (WDX) spectroscopy. The more insulating AlN-rich layers were measured by Rutherford backscattering spectrometry (RBS). The $\text{Al}_{0.31}\text{Ga}_{0.69}\text{N}$ sample was measured by both techniques with very similar results. High-resolution photoluminescence (PL) spectra were taken at 15 K in the vicinity of the $^5\text{D}_0\text{-}^7\text{F}_2$ transition (~ 622 nm in GaN) by using monochromated light from a 1 kW Xe lamp; PL excitation (PLE) spectra were obtained by monitoring selected lines of this transition while scanning the excitation wavelength. All PLE spectra were corrected for the spectral response of the Xe lamp and monochromator.

III. EXPERIMENTAL RESULTS

Figure 1 plots PL spectra in the region of the $^5\text{D}_0\text{-}^7\text{F}_2$ transition for nine samples, normalized to the intensity of the highest peak. For two samples two PL spectra are shown, corresponding to excitation across and below the band gap. In the other cases the excitation wavelengths used were those of the $\text{Al}_x\text{Ga}_{1-x}\text{N}$ band gaps, as determined by PLE spectra, except for the AlN (excited by 325 nm wavelength laser light) and $\text{Al}_{0.98}\text{Ga}_{0.02}\text{N}$ (excited by the Xe lamp at 345 nm). PL spectra of all the samples also feature a broad UV band (not shown) with an integrated PL intensity roughly equal to the sum of *all* the visible sharp-line emissions. The peak of this band, ~ 3.26 eV in GaN:Eu, shifts to higher energy as *x* increases. As described in Refs. 19–21 and shown in Fig. 1, two distinct Eu spectra occur when GaN:Eu is excited above

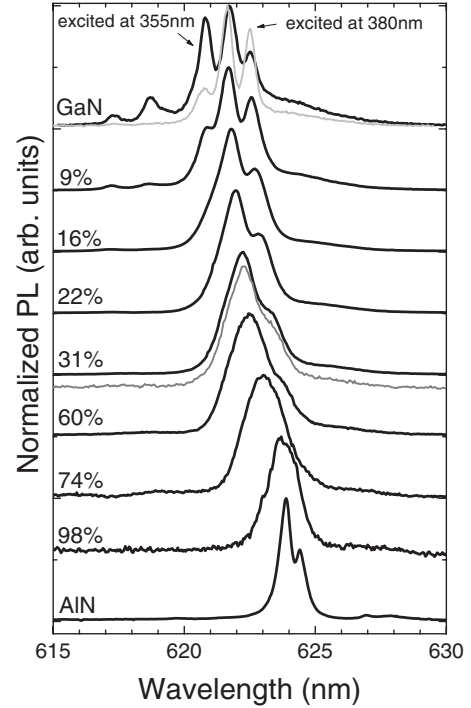


FIG. 1. High-resolution 15 K PL spectra of the $^5\text{D}_0\text{-}^7\text{F}_2$ transition of implanted $\text{Al}_x\text{Ga}_{1-x}\text{N}:\text{Eu}$ for the whole alloy composition range. For GaN and $\text{Al}_{0.31}\text{Ga}_{0.69}\text{N}$, spectra obtained for excitation both above gap and at the peak of the X_1 PLE feature are shown.

and below the band edge. Selectively excited spectra for $\text{Al}_{0.07}\text{Ga}_{0.93}\text{N}:\text{Eu}$ are shown in Fig. 2(a) and demonstrate a similar situation, indicative of at least two Eu centers in these samples. The peak at 620.8 nm is clearly observed for exci-

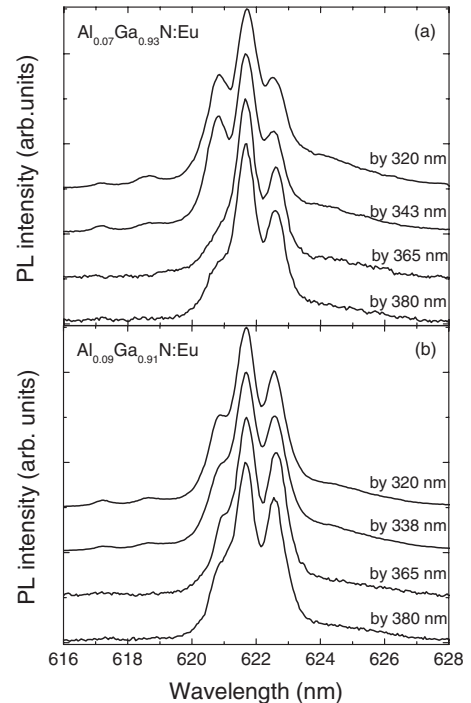


FIG. 2. Selectively excited 15 K PL spectra of Eu $^5\text{D}_0\text{-}^7\text{F}_2$ emission for (a) $\text{Al}_{0.07}\text{Ga}_{0.93}\text{N}:\text{Eu}$ and (b) $\text{Al}_{0.09}\text{Ga}_{0.91}\text{N}:\text{Eu}$.

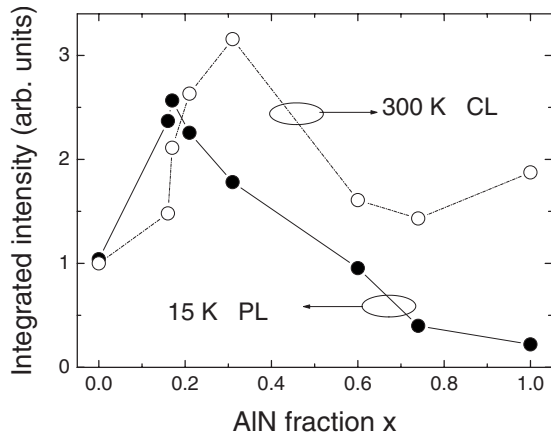


FIG. 3. The integrated 15 K PL (left) and 300 K CL (right) intensity of ${}^5\text{D}_0\text{-}{}^7\text{F}_2$ transition of Eu luminescence from 615 to 630 nm as a function of AlN fraction.

tation at energies at or above the band edge (343 nm) but its intensity is decreased dramatically for subgap excitation (e.g., 365 or 380 nm). Figure 2(b) shows a similar situation for $\text{Al}_{0.09}\text{Ga}_{0.91}\text{N}:\text{Eu}$, although the decrease in intensity of the extra line is less pronounced. However, for all $\text{Al}_x\text{Ga}_{1-x}\text{N}$ hosts with $x > 0.15$, excitation above or below the band-edge results in almost identical spectral patterns. Additional lines seen for $0 < x < 0.15$ samples resemble those excited only by above band-gap light in GaN. Finally annealing $\text{Al}_x\text{Ga}_{1-x}\text{N}:\text{Eu}$ with $x > 0.15$ at high temperatures strongly influences the line intensities but does not alter the spectral patterns. In the case of GaN:Eu, the two dominant Eu centers have very different annealing dependences.²⁰ These observations are all consistent with the presence in $\text{Al}_x\text{Ga}_{1-x}\text{N}$ samples with $x > 0.15$ of a single luminescent Eu center, which can be excited both above and below the host band gap. The Eu center in GaN excited by light both below and above the band gap, which will be referred to as Eu_I , is dominant in $\text{Al}_x\text{Ga}_{1-x}\text{N}$ with $x > 0.15$ and appears to be the same as that found in GaN annealed at low temperature. The additional Eu luminescence spectrum (Eu_{II}) found in $\text{Al}_x\text{Ga}_{1-x}\text{N}$ samples with $x < 0.15$ can *only* be excited above the gap and becomes dominant in GaN samples annealed at higher temperatures.^{20,21}

Figure 3 shows the integrated PL and CL intensities as a function of AlN fraction, normalized to that of GaN:Eu. The PL spectra were obtained by excitation at the band edge (except for AlN:Eu, which is excited at 350 nm) and the resulting intensity adjusted according to the intensity of the incident excitation light. The intensity increases in the low Al content region and reaches a maximum at around $x = 0.2\text{--}0.3$. In Ref. 4 Wakahara *et al.* observed an increase in more than one order of magnitude for $\text{Al}_{0.4}\text{Ga}_{0.7}\text{N}:\text{Eu}$ compared to GaN:Eu and a decrease for $x > 0.4$. Our results show a maximum intensity increase of about ~ 3 times compared to GaN:Eu for both 15 K PL and 300 K CL. It should be pointed out that our samples were annealed at 1300 °C while those in Ref. 4 were annealed at 1100 °C, which could account for the different rates of increase.

The linewidths of the component lines of the ${}^5\text{D}_0\text{-}{}^7\text{F}_2$ emission multiplet show marked variations (Fig. 1) with

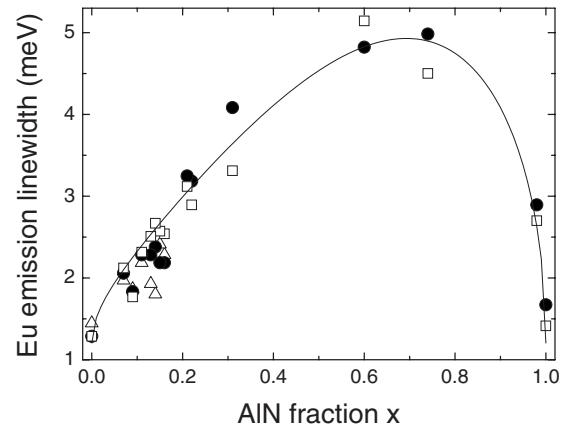


FIG. 4. FWHM of the main emission lines of the Eu ${}^5\text{D}_0\text{-}{}^7\text{F}_2$ transition as a function of AlN molar fraction. The triangles, circles, and squares correspond to the lower, central, and upper wavelength lines of the PL “triplet,” respectively. The solid line is described in the text and is a fit to the circular data points.

composition. In order to extract the component linewidths, the emission spectra were decomposed into two or three Lorentzians, depending on the value of x . Figure 4 plots the full width at half maximum (FWHM) of the fitted components as a function of AlN fraction. The asymmetrical variation in linewidth as a function of composition is strongly reminiscent of that observed for bound excitons in semiconductor alloys.²² We fit to the extracted linewidth data an expression adapted from that derived in Ref. 23

$$\sigma(x) = \sigma_0 + \frac{dE_g(x)}{dx} \sqrt{\frac{8 \ln(2)x(1-x)}{(4\pi/3)R_{\text{ex}}^3 K}}, \quad (1)$$

where K is the cation/anion number density, $\sqrt{2/a_0^3}$ for the wurtzite lattice with $a_0 = 3.15 \text{ \AA}$ the average a -plane lattice constant (for simplicity). The residual linewidth, σ_0 , is taken to be 1.4 meV for all samples. RBS estimates of residual lattice disorder, to be published elsewhere, confirm this assumption. The fit is seen to be exceptionally good with small scatter in the component linewidths for a given composition. Using experimental band gaps and bowing parameter of $E_g(\text{GaN}, \text{AlN}) = 3.5 \text{ eV}$, 6.2 eV and $b = -1.5 \text{ eV}$ to determine dE_g/dx , we estimate a mean exciton radius, R_{ex} , of $\sim 10 \text{ nm}$. More important than this magnitude is the fact that the asymmetric dependence of linewidth on x shows the influence of alloy disorder through the binomial term in Eq. (1) with an energy scaling that depends only on the bowing parameter, b . Similar broadening is observed in spectra of $\text{Al}_x\text{Ga}_{1-x}\text{N}:\text{Dy}$,¹⁴ which also shows a small upshift in peak energy, in $\text{Al}_x\text{Ga}_{1-x}\text{N}:\text{Tm}$,¹⁴ which has no measurable peak shift, and in $\text{Al}_x\text{Ga}_{1-x}\text{N}:\text{Pr}$.¹⁵ These observations suggest an excitonic nature of Eu, Pr, Dy, and Tm emissions in $\text{Al}_x\text{Ga}_{1-x}\text{N}$. The maximum broadening of $\text{Al}_x\text{Ga}_{1-x}\text{N}:\text{Eu}$ emission lines ($\sim 3.5 \text{ meV}$ at $x \sim 0.75$) is ~ 10 times smaller than that of band-edge excitons.²³ For such excitons, the emission energy is naturally associated with the optical band gap; but the *peak* energy of the ${}^5\text{D}_0\text{-}{}^7\text{F}_2$ transition is almost independent of the host composition: it decreases by only 7 meV between GaN and AlN. We note that a strikingly similar

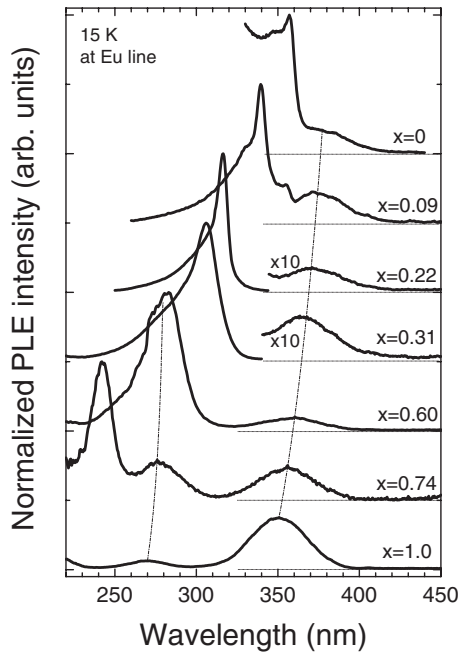


FIG. 5. 15 K PLE spectra of $\text{Al}_x\text{Ga}_{1-x}\text{N}:\text{Eu}$ detected at the peak of the ${}^5\text{D}_0\text{-}{}^7\text{F}_2$ luminescence, apart from the case of GaN for which the long-wavelength line was used. All spectra, except AlN, were normalized to the band-edge peak. The dashed lines are guides for the eye, charting the evolution of the X_1 and X_2 features.

asymmetry of the magnetic moment of $\text{Al}_x\text{Ga}_{1-x}\text{N}:\text{Tm}$ has been recently reported by Nepal *et al.*²⁴

Figure 5 compares PLE spectra of $\text{Al}_x\text{Ga}_{1-x}\text{N}:\text{Eu}$ samples, detected at the strongest peak of the ${}^5\text{D}_0\text{-}{}^7\text{F}_2$ luminescence apart from that for GaN, for which the longer wavelength peak at 622.5 nm was used to avoid mixing in of the second Eu component. The PLE spectra are normalized to the excitation peak at the band edge, except in the case of AlN, for which the band-edge onset near 200 nm (6.2 eV) is beyond reach of our excitation lamp. All spectra show at least one “below-gap” excitation band, whose peak energy upshifts linearly with increasing x as plotted in Fig. 6. The shift, from 3.26 eV for GaN to 3.54 eV for AlN, is only a tenth of the band-gap widening. As a consequence the excitation feature, which we label X_1 , lies close to the band edge in GaN but approaches mid gap in AlN. For low AlN fractions, X_1 overlaps the strong band-edge absorption but it is resolved even for GaN. Its FWHM is approximately constant with a value near 0.4 eV across the whole composition range. As the AlN fraction increases, a second feature (X_2 on Fig. 6), with a similar FWHM to X_1 , emerges below the shifting gap at $x \sim 0.6$. Eu in $\text{Al}_x\text{Ga}_{1-x}\text{N}$ thus introduces two excitation bands, both of which may lead to Eu^{3+} PL.

IV. DISCUSSION

In the absence of microscopic information on defect structure, we shall provide a description of the $X_{1,2}$ bands as *excitonic* features associated with a specific Eu center. In light of similar PLE data from a wide range of different samples it can be seen that the involvement of “sensitizing

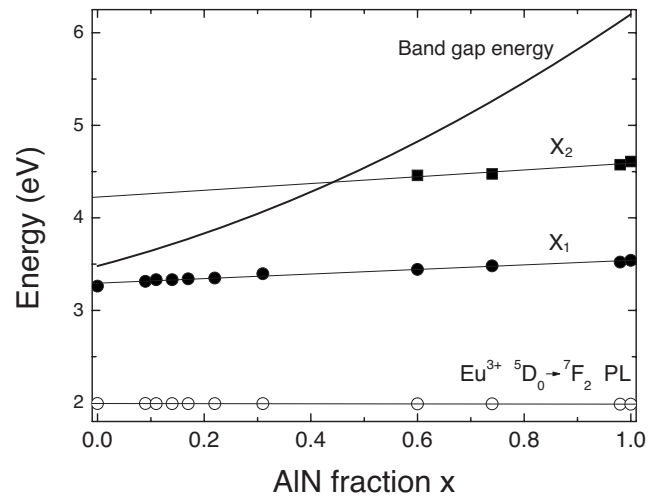


FIG. 6. Excitation energies of $\text{Al}_x\text{Ga}_{1-x}\text{N}:\text{Eu}$ derived from PLE as a function of AlN molar fraction. Open circles correspond to the PL used to monitor the excitation spectra.

defects” in the excitation process is an unnecessary complication. Furthermore the obvious candidate species, the native lattice defects and point defects created during implantation, would lead to much stronger shifts in energy of $X_{1,2}$ with composition due to the strong valence- or conduction-bandlike character of their associated states. By trapping an exciton, this particular Eu center can act as its own sensitizer. Many, perhaps all, RE-doped wide band-gap solids feature strong UV absorption peaks, as identified as X_1 in this work, which are usually assigned to “electrons... excited from a neighboring anion orbital onto the dopant ion.”²⁵ In the language of semiconductor physics, such electron transfer produces a core exciton, favored by the strong exciton binding energy in wide gap III nitrides. A number of different atomic states can be considered for the localized electron but the charge-transfer state is in any case analogous to a core exciton on account of the separated electron and hole which enhance the oscillator strength of the transition. A charge transfer into the empty $5d$ shell of the RE is a strong candidate, leaving the $4f$ optical core states of the RE essentially unchanged. Such an entity will be referred to as a d exciton. The excess energy in this d exciton can then be transferred to the $4f$ shell leading to the characteristic sharp-line RE^{3+} emission. At the same time, the UV emission band, mentioned previously, may be ascribed to recombination of d excitons. The anomalous loss, in the context of the Favenne rule, of luminescence efficiency of the sharp lines at high values of x reflects the emergence of X_2 , whose higher energy opens the possibility of extra energy losses between excitation and emission.

The general form of the fitting used in Eq. (1) applies to a state with sufficient spatial extent to sample the composition fluctuations of an alloy and therefore be sensitive to the band-gap variation in the alloy. If variations in the crystal field, due to local compositional fluctuations, were responsible for broadening the line, the variation in linewidth might be expected to be symmetric about $x=0.5$. For ordinary alloy excitons, the transition energy can be very closely identified with the band gap; this is obviously not true for the ${}^5\text{D}_0\text{-}{}^7\text{F}_2$

PL component lines, which shift by only 7 meV between GaN and AlN. (Dy- and Tm-related PL lines in $\text{Al}_x\text{Ga}_{1-x}\text{N}$ shift by even smaller amounts but still broaden considerably). Figure 4 demonstrates that a spatially extended state is involved in the $^5\text{D}_0$ - $^7\text{F}_2$ luminescence, associated with the de-excitation of the extended d exciton.

This exciton picture, combined with the estimated “exciton” size implies that these centers are closer in character to isoelectronic exciton traps^{10,26} than a defect perturbed by a crystal field. Unlike conventional isoelectronic centers, however, the complexities of the rare-earth electron configuration must also be considered.¹⁰ Additionally the presence of the X_2 excitation band must still be explained. Lozykowski and Jadwisienczak²⁶ have argued that clustering of RE ions is responsible for a series of PLE features, which would correspond to a series of excitation features $X_{1,2,\dots,m}$; however such clustering would lead to characteristic features in the emission spectra of some RE ions²⁷ and we still have the problem of excitation transfer from cluster to single ion to contend with. Moreover, EXAFS studies of GaN:Eu, even at rather large doping levels, showed only isolated Eu_{Ga} .⁷ The host independent, and almost RE independent, X-band energies suggest an alternative origin, as the $5d^1$ configuration splits into high and low spin states, separated by ~ 1 eV according to Ref. 8.

The second luminescent Eu site (Eu_{II}), which appears in the low AlN content ($x < 0.15$) $\text{Al}_x\text{Ga}_{1-x}\text{N}$ samples, is not excited via the X bands. The detailed spectroscopy of this site is the subject of on-going studies. It is important to comment on the above hypotheses with relation to the possibility of direct excitation of higher-lying $4f$ levels as reported in Ref. 16, where higher-lying Tm^{3+} levels gave a broad, structured band in the excitation spectra. The general occurrence of X_1 type bands in the UV region has been noted for a variety of REs (Refs. 14, 15, and 25) but Dieke-type energy-level diagrams for ions other than Tm indicate that similar

sets of higher RE levels at the necessary energies are not generally available. Furthermore the data in this present report describe the dependence of the energy of the X_1 and X_2 bands on host composition and show a considerably larger shift (≈ 300 meV or more) than expected for RE levels within a given host or when compared to the composition dependence of the $^5\text{D}_0$ - $^7\text{F}_2$ transition. Considering also the lack of structure in our X_1 and X_2 excitation bands we conclude that direct RE excitation could not explain the data in this case.

V. CONCLUSION

In summary, we have presented PL and PLE data over the whole composition range of $\text{Al}_x\text{Ga}_{1-x}\text{N}$ doped with Eu. One dominant Eu center can be excited by both above and below gap excitation, leading to PL with component linewidths characteristic of an excitonic extended state. The excitation path of Eu is found to be largely insensitive to the composition, showing a comparatively small shift in energy and is identified as the creation of d excitons. The characteristic sharp-line RE^{3+} emission then follows transfer of the excess energy in this d exciton to the $4f$ shell. Intriguingly, certain other Eu centers, found in GaN and in GaN-rich $\text{Al}_x\text{Ga}_{1-x}\text{N}$, have a completely different excitation mechanism.

ACKNOWLEDGMENTS

We thank P. J. Parbrook and T. Wang (University of Sheffield) for supplying the $\text{Al}_{0.98}\text{Ga}_{0.02}\text{N}$ sample and R. Vianden (University of Bonn) for RTA facilities. We acknowledge funding from the Royal Society of Edinburgh BP Research Fund (B.H.) and FCT, Portugal (POCI/FIS/57550/2004). We thank P. Dorenbos and H. Lozykowski for copies of their work and G. Davies and A. Efros for insightful comments during the preparation of the original version of this paper.

*Present address: Department of Photonics, School of Science and Engineering, Ritsumeikan University, 1-1-1 Noji-Higashi, Kusatsu-shi, Shiga 525-8577, Japan.

¹H. Ennen, J. Schneider, G. Pomrenke, and A. Axmann, *Appl. Phys. Lett.* **43**, 943 (1983).

²P. N. Favennec, H. L’Haridon, M. Salvi, D. Moutonnet, and Y. Le Guillou, *Electron. Lett.* **25**, 718 (1989).

³A. J. Steckl, J. C. Heikenfeld, D. S. Lee, M. J. Garter, C. C. Baker, Y. Q. Wang, and R. Jones, *IEEE J. Sel. Top. Quantum Electron.* **8**, 749 (2002); J. H. Park and A. J. Steckl, *Appl. Phys. Lett.* **85**, 4588 (2004).

⁴A. Wakahara, *Opt. Mater.* **28**, 731 (2006).

⁵D. S. Lee and A. J. Steckl, *Appl. Phys. Lett.* **83**, 2094 (2003).

⁶U. Hömmerich, E. E. Nyein, D. S. Lee, A. J. Steckl, and J. M. Zavada, *Appl. Phys. Lett.* **83**, 4556 (2003).

⁷K. P. O’Donnell and B. Hourahine, *Eur. Phys. J.: Appl. Phys.* **36**, 91 (2006).

⁸B. Judd, *Phys. Rev.* **127**, 750 (1962); G. Ofelt, *J. Chem. Phys.* **37**, 511 (1962).

⁹P. Dorenbos and E. van der Kolk, *Opt. Mater.* **30**, 1052 (2008); *Proc. SPIE* **6473**, 647313 (2007).

¹⁰H. J. Lozykowski, W. M. Jadwisienczak, A. Bensaoula, and O. Monteiro, *Microelectron. J.* **36**, 453 (2005); H. J. Lozykowski, *Phys. Rev. B* **48**, 17758 (1993).

¹¹C. W. Lee, H. O. Everitt, D. S. Lee, A. J. Steckl, and J. M. Zavada, *J. Appl. Phys.* **95**, 7717 (2004).

¹²S. Kim, S. J. Rhee, D. A. Turnbull, X. Li, J. J. Coleman, S. G. Bishop, and P. B. Klein, *Appl. Phys. Lett.* **71**, 2662 (1997).

¹³S. Petit, R. Jones, M. J. Shaw, P. R. Briddon, B. Hourahine, and T. Frauenheim, *Phys. Rev. B* **72**, 073205 (2005).

¹⁴I. M. Roqan, K. P. O’Donnell *et al.* (unpublished).

¹⁵M. Peres, S. Magalhães, N. Franco, M. J. Soares, A. J. Neves, E. Alves, K. Lorenz, and T. Monteiro, *Microelectron. J.* **40**, 377 (2009).

¹⁶Y. D. Glinka, H. O. Everitt, D. S. Lee, and A. J. Steckl, *Phys. Rev. B* **79**, 113202 (2009).

¹⁷T. Wang, J. Bai, P. J. Parbrook, and A. G. Cullis, *Appl. Phys. Lett.* **87**, 151906 (2005).

- ¹⁸K. Lorenz, U. Wahl, E. Alves, S. Dalmaso, R. W. Martin, K. P. O'Donnell, S. Ruffenach, and O. Briot, *Appl. Phys. Lett.* **85**, 2712 (2004).
- ¹⁹K. Wang, R. W. Martin, K. P. O'Donnell, V. Katchkanov, E. Nogales, K. Lorenz, E. Alves, S. Ruffenach, and O. Briot, *Appl. Phys. Lett.* **87**, 112107 (2005).
- ²⁰K. Wang, R. W. Martin, E. Nogales, V. Katchkanov, K. P. O'Donnell, S. Hernandez, K. Lorenz, E. Alves, S. Ruffenach, and O. Briot, *Opt. Mater.* **28**, 797 (2006).
- ²¹L. Bodiou, A. Oussif, A. Braud, J.-L. Doualan, R. Moncorgé, K. Lorenz, and E. Alves, *Opt. Mater.* **28**, 780 (2006).
- ²²E. F. Schubert, E. O. Gobel, Y. Horikoshi, K. Ploog, and H. J. Queisser, *Phys. Rev. B* **30**, 813 (1984).
- ²³A. N. Westmeyer, S. Mahajan, K. K. Bajaj, J. Y. Lin, H. X. Jiang, D. D. Koleske, and R. T. Senger, *J. Appl. Phys.* **99**, 013705 (2006).
- ²⁴N. Nepal, S. M. Bedair, N. A. El-Masry, D. S. Lee, A. J. Steckl, and J. M. Zavada, *Appl. Phys. Lett.* **91**, 222503 (2007).
- ²⁵B. Henderson and G. F. Imbusch, *Optical Spectroscopy of Inorganic Solids* (Clarendon, Oxford, 1989), p. 404.
- ²⁶H. J. Lozykowski and W. M. Jadwisieniczak, *Phys. Status Solidi B* **244**, 2109 (2007).
- ²⁷L. Bodiou, A. Braud, C. Terpin, J. L. Doualan, R. Moncorgé, K. Lorenz, and E. Alves, *J. Lumin.* **122-123**, 131 (2007).